Quantum theory of elementary excitations on semiconducting surfaces and in low-dimensional-electronic systems

by Hong Yu

A thesis submitted in partial fulfillment of the requirements for the degree Doctor of Philosophy
Physics
Montana State University

Abstract:
We discuss plasmon and phonon excitations in the accumulation layer of a semiconductor with the aid of calculations based on a nonlocal description of dynamical density response in the random-phase-approximation. The first model considered is that of a polarizable jellium slab at finite temperature with surface charges that bend the conduction bands downwards; lattice vibrations are ignored. Choosing model parameters appropriate to lightly doped InAs(110) at room temperature, and to ZnO accumulation layers at low temperature, we obtain intersubband as well as intrasubband plasmons and discuss their dispersion relations, localizations, and line shapes. Evidence for two-dimensional and "acoustic" plasmon is presented. All plasmon modes are strongly damped when their dispersion curves enter the single-particle continua. When the dynamical response of the lattice is included in the model, we obtain coupled plasmon-phonon modes or "plasmarons" and study their dispersion and line shapes.

Self-consistent calculations of the subband electronic structure as well as the single-particle and collective excitations of semiconductor quantum wires are, for the first time, presented. Calculated energy levels, wavefunctions, charge density and potential for the quantum wire in the GaAs/A1GaAs heterostructure differ from the predictions of the simple particle-in-a box model because of the influence of accumulation and depletion regions. The dynamical structure factor, evaluated in the random-phase-approximation, displays unique line shapes and dispersion relations which are in sharp contrast with the results expected for higher-dimensional electron gases. A well defined spectral feature is attributed to an acoustic plasmon. The calculated intersubband resonance frequency of the quantum wire, shifted upward by the depolarization field, agrees well with previous experiments.

QUANTUM THEORY OF ELEMENTARY EXCITATIONS ON SEMICONDUCTING SURFACES AND IN LOW-DIMENSIONAL-ELECTRONIC SYSTEMS

by

Hong Yu

A thesis submitted in partial fulfillment
of the requirements for the degree

of

Doctor of Philosophy

in

Physics

MONTANA STATE UNIVERSITY
Bozeman, Montana

August, 1990

APPROVAL

of a thesis submitted by

Hong Yu

This thesis has been read by each member of the thesis committee and has been found to be satisfactory regarding content, English usage, format, citations, bibliographic style, and consistency, and is ready for submission to the College of Graduate Studies.

8-16-90
Date

Chairperson, Graduate Committee

Approved for the Major Department

8-16-90
Date

Head, Major Department

Approved for the College of Graduate Studies

9/4/90
Date

Graduate Dean

STATEMENT OF PERMISSION TO USE

In presenting this thesis in partial fulfillment of the requirements for a doctoral degree at Montana State University, I agree that the Library shall make it available to borrowers under rules of the Library. I further agree that copying of this thesis is allowable only for scholarly purposes, consistent with "fair use" as prescribed in the U. S. Copyright Law. Requests for extensive copying or reproduction of this thesis should be refered to University Microfilms International, 300 North Zeeb Road, Ann Arbor, Michigan 48106, to whom I have granted "the exclusive right to reproduce and distribute copies of the dissertation in and from microfilm and the right to reproduce and distribute by abstract in any format."

Signature 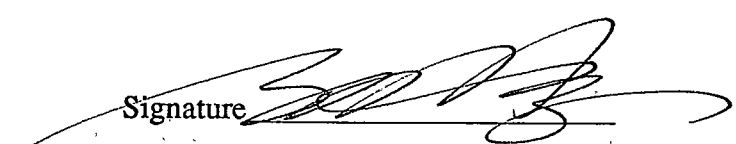

Date 8-16-90

ACKNOWLEDGEMENTS

My deepest acknowledgements go to my advisor, Dr. John C. Hermanson, for his guidance, timely suggestions, patient discussions, and for his friendship.

It is difficult to acknowledge all the people who have contributed encouragement to me in order to complete this thesis. I would like to thank Dr. Gerald J. Lapeyre for many useful discussions.

Among the numerous people who have helped me to make this thesis reality, it is the best to acknowledge my parents for the love and support they have given. I would especially like to thank my wife, Ting, for her supreme effort which she has taken during the past six years. Her love and support have made the hard work much more bearable. Thank you, Ting.

Financial support for the work was from NSF grant DMR-87-05879.

TABLE OF CONTENTS

Page

APPROVAL....ii
STATEMENT OF PERMISSION TO USE....iii
ACKNOWLEDGEMENTS....iv
TABLE OF CONTENTS....v
LIST OF TABLES....vii
LIST OF FIGURES....viii
ABSTRACT.... x

CHAPTER 1. INTRODUCTION....1

CHAPTER 2. GENERAL THEORY OF ELEMENTARY EXCITATIONS OF AN INHOMOGENEOUS ELECTRON GAS....2

Introduction....2
Electron Energy Loss Function....4
Dynamical Structure Factor....8
Density Reponse Function....9
Random Phase Approximation....11
Single Particle (Spin Density) Excitations and Collective (Charge Density) Excitations....13

CHAPTER 3. ELECTRONIC SUBBAND STRUCTURE AND PLASMON EXCITATIONS OF A QUASI-TWO-DIMENSIONAL ELECTRON GAS....16

Introduction....16
Accumulation Layers on InAs(110)....18

TABLE OF CONTENTS-----Continued

Model and RPA Formalism.....18
Results and Discussion.....24
Comparison with HREELS Data.....35
Accumulation Layers on ZnO.....50
Subband Electronic Structure.....50
Dynamics of the Electron Gas.....59
Plasmon-Phonon Coupling.....65

CHAPTER 4. ELECTRONIC SUBBAND STRUCTURE AND DYNAMICS OF QUASI-ONE-DIMENSIONAL ELECTRON SYSTEMS.....74

Introduction.....74
Model and Self-Consistent Formalism for a Q1DEG.....75
Results and Discussion of Electronic Subband Properties.....80
Dynamical Structure Factor of a Quantum Wire in the RPA.....88

CHAPTER 5. CONCLUSIONS.....98

REFERENCES CITED.....100

LIST OF TABLES

Page

1. Comparison with Experimental Data.....87

LIST OF FIGURES

Page

1. Illustration of electronic excitations in quasi-two-dimensional electron gas.....17
2. Self-consistent surface charge density and potential of InAs accumulation layer.....25
3. Electron-energy loss functions (without phonon) with different momentum transfer...27
4. Induced charge density at plasmon resonance frequencies.....29
5. Induced potential at plasmon resonance frequencies.....30
6. Dispersion relations of inter- and intra-subband plasmon modes.....32
7. Electron-energy loss functions (without phonon) with different surface charge densities.....36
8. Plasmon resonance frequencies vs. surface charge density.....37
9. Electron-energy loss functions (with phonon) with different momentum transfer.....38
10. Electron-energy loss functions (with phonon) with different surface charge densities.40
11. Dispersion relations of plasmaron modes.....41
12. Experimental HREELS data with different hydrogen exposure.....42
13. Experimental HREELS data with different primary energy of electron beam.....45
14. Calculated HREELS spectra without instrumental broadening.....47
15. Calculated HREELS spectra with instrumental broadening.....48
16. Calculated HREELS spectra with different surface charge densities.....49
17. Model of ZnO slab.....52
18. Self-consistent charge density and potential of ZnO accumulation layer.....55
19. Self-consistent charge densities with different parameters.....57
20. Subband properties as a function of surface charge density.....58
21. Electron-energy loss functions with different momentum transfer.....61
22. Dispersion relations of inter- and intra-subband plasmons for ZnO.....63
23. Induced charge density as a function of frequency and distance inside ZnO surface...64

LIST OF FIGURES-----Continued

24. Electron-energy loss function and dispersion relation of plasmaron modes.....67

25. Electron-energy loss function and dispersion relation of plasmaron modes.....69

26. Calculated HREELS spectra with different primary energy for ZnO surface.....70

27. Calculated inter-subband HREELS spectra with different incidence angle.....71

28. Model of quantum wire.....76

29. Wave functions of the lowest four subband in the quantum wire.....81

30. Self-consistent charge density and potential of the quantum wire.....84

31. Subband energy levels as a function of wire charge density.....86

32. dynamical structure factor.....94

33. Dispersion relations of elementary excitations in the quantum wire.....96

ABSTRACT

We discuss plasmon and phonon excitations in the accumulation layer of a semiconductor with the aid of calculations based on a nonlocal description of dynamical density response in the random-phase-approximation. The first model considered is that of a polarizable jellium slab at finite temperature with surface charges that bend the conduction bands downwards; lattice vibrations are ignored. Choosing model parameters appropriate to lightly doped InAs(110) at room temperature, and to ZnO accumulation layers at low temperature, we obtain intersubband as well as intrasubband plasmons and discuss their dispersion relations, localizations, and line shapes. Evidence for two-dimensional and "acoustic" plasmon is presented. All plasmon modes are strongly damped when their dispersion curves enter the single-particle continua. When the dynamical response of the lattice is included in the model, we obtain coupled plasmon-phonon modes or "plasmarons" and study their dispersion and line shapes.

Self-consistent calculations of the subband electronic structure as well as the single-particle and collective excitations of semiconductor quantum wires are, for the first time, presented. Calculated energy levels, wavefunctions, charge density and potential for the quantum wire in the GaAs/AlGaAs heterostructure differ from the predictions of the simple particle-in-a box model because of the influence of accumulation and depletion regions. The dynamical structure factor, evaluated in the random-phase-approximation, displays unique line shapes and dispersion relations which are in sharp contrast with the results expected for higher-dimensional electron gases. A well defined spectral feature is attributed to an acoustic plasmon. The calculated intersubband resonance frequency of the quantum wire, shifted upward by the depolarization field, agrees well with previous experiments.

CHAPTER 1

INTRODUCTION

During the past ten years the basic understanding of collective excitations near semiconductor surfaces and interfaces has been deepened through a variety of both experimental and theoretical studies. On the experimental side, several investigations of surface phonons and plasmons in doped semiconductor have been carried out by means of high-resolution-electron-energy-loss spectroscopy(HREELS)[1-7]. HREELS is a particularly useful probe of these excitations because its effective sampling depth is on the order of the width of the space-charge region, namely about 100 Å. Thus the energy-loss spectrum provides important infomation on the dynamics of an inhomogeneous electron gas.

Until recently, HREELS investigations of plasmon-phonon modes at semiconductor surfaces have been confined to depletion layers. Although collective excitations have been observed in the accumulation layer of the insulator ZnO[8], studies of an accumulation layer formed on a free semiconductor surface were lacking until now. Mills and his co-workers have performed theoretical studies of surface plasmons on both depletion and accumulation layers on GaAs surface at room temperature[9-12], using a nonlocal dielectric response formalism in the random-phase-approximation(RPA). Exploiting the RPA formalism, Ehlers[13] performed calculations of surface plasmons in GaAs accumulation layers at various temperatures. His results indicate that at low temperature two-dimensional plasmon behavior[14] becomes manifest in this material, owing to the factor that only the lowest few subbands have siginificant population. Chen *et al.*[15]have reported studies of collective excitations in InAs(110) accumulation layers. Finally, Yu and Hermanson[16] studied the InAs(110) accumulation layers at room temperature by the dynamical-linear-density-response theory of the conduction electrons

within the RPA, based on the knowledge of the electronic subband structure which was determined by a self-consistent-field method. We found evidence of 2D and acoustic plasmons in the InAs(110) accumulation layer. Our results included the dispersion relations, spatial localizations, and line shapes of intersubband as well as intrasubband plasmons. When the phonon excitations were included, we obtained coupled plasmon-phonon modes or "plasmarons". A more detailed calculation on a strong accumulation ZnO layer was also reported by us[17]. Because of the strong localization of the conduction electrons near the surface (a length scale of about 10Å), microscopic details usually ignored in space-charge layers, such as quantum tunneling into the surface barrier, position dependence of the effective mass, and exchange and correlation effects[18] were taken into account. Some of the excitation modes we found have not yet been observed in experiments.

One-dimensional electron systems have attracted considerable interest following advances in high-resolution lithography which have made it possible to fabricate semiconductor structures that confine the motion of electrons in two directions. This confinement gives rise to quasi-one-dimensional electronic properties. The behavior of the quasi-one-dimensional electron gas is expected to be different dramatically from that of its higher-dimensional counterpart.

CHAPTER 2

GENERAL THEORY OF ELEMENTARY EXCITATIONS OF AN INHOMOGENEOUS ELECTRON GAS

Introduction

The interaction between an external electron-beam probing and an inhomogeneous electron gas such as that found in space-charge layers in semiconductors can be separated into two regimes. One is the so called dipole scattering regime, in which the electrons are scattered by the dipole field generated by charge density fluctuations in the electron gas into a very narrow cone with an axis along the specular direction; thus the momentum transfer parallel to the surface is very small. The modes excited in this regime are the highly surface localized phonons and collective excitations due to long range correlations in the medium[19,20]. The other regime is the impact scattering regime where the electrons are scattered by the local atomic or molecular field. The signature of such an interaction is a large momentum transfer parallel to the surface; thus the behavior of the excitation in the medium is single-particle like[19,20]. HREELS spectra are usually collected along the specular direction, and thus they reflect the physical properties within the dipole scattering regime. HREELS has been revealed to be a very powerful technique for the study of surface modes of semiconductors including collective excitations.

Theoretically, in the first Born approximation, the scattering efficiency is proportional to the loss function $P(\mathbf{q},\omega)$[21-23] or, equivalently, the dynamical structure factor $S(\mathbf{q},\omega)$[24]; these are the two most important functions in studying the scattering process due to the richness of the physical information contained in them. The energy-loss

function and the dynamical structure factor are closely related to the density response function $\chi(\mathbf{r},\mathbf{r}';\omega)$. To determine $\chi(\mathbf{r},\mathbf{r}';\omega)$ in the random-phase-approximation, an integral equation has to be solved numerically. The main purpose of the following few sections is to address the details of the theoretical determination of the scattering efficiency which is directly comparable with the HREELS spectrum.

Electron Energy Loss Function

In a high-resolution electron-energy-loss experiment, a highly monochromatic electron beam with energy E_I and momentum $\mathbf{q}_I(\hbar=1)$ impinges on the solid surface, and the scattered electrons of energy E_S and momentum $\mathbf{q}_S$ are collected by an analyzer. In the scattering process the electron energy loss ω and momentum transfer $\mathbf{q}_{\|}$ are conserved: $E_S=E_I-\omega$ and $\mathbf{q}_S=\mathbf{q}_I-\mathbf{q}_{\|}$ (the last subscript denotes the parallel to the surface).

The resulting near-specular scattering process can be described by the scattering efficiency per unit frequency, $ds/d\omega$, which is the probability that an electron will be scattered from its initial state into a final state with an energy loss between ω and $\omega+d\omega$. The quantity may be written as [10,12,25,26]

$$\frac{ds}{d\omega}=\frac{2e^2v_\perp^2}{\pi\hbar}\int d^2\vec{q}_{\|}\frac{P(\vec{q}_{\|},\omega)}{[v_\perp^2q_{\|}^2+(\omega-\vec{v}_{\|}\cdot\vec{q}_{\|})^2]^2}, \qquad (1)$$

where $v_\perp$ and $v_{\|}$ are the components of the incident electron's velocity perpendicular and parallel to the surface. In the above equation $P(q_{\|},\omega)$ is the so called frequency and wavevector-dependent energy-loss function.

Let us imagine the semiconductor medium with dielectric constant ε is located in the half-space $z > 0$ and describe the external charge's trajectory by

$$\vec{R}(t) = (v_{\|}t, v_{\perp}|t|), \tag{2}$$

where $v_{\|}$ and $v_{\perp}$ are defined above. The perturbing potential felt by the semiconductor is[27]

$$\phi_{ext}(\vec{r},t) = \frac{-2e}{(1+\varepsilon)[\vec{r}-\vec{R}(t)]}, \tag{3}$$

or [23,28,29], after Fourier transformation,

$$\phi_{ext}(q_{\|},\omega;z) = \frac{8\pi e^2 v_{\perp} e^{-q_{\|}z}}{(1+\varepsilon)[q_{\|}^2 v_{\perp}^2 + (\omega - \vec{q}_{\|}\cdot\vec{v}_{\|})^2]}. \tag{4}$$

To return to the general discussion, we relate an essential quantity, the so-called induced charge density $n_{ind}(\mathbf{r},\omega)$, to $\chi^0(\mathbf{r},\mathbf{r};\omega)$ and $\chi(\mathbf{r},\mathbf{r};\omega)$, which are the non-interacting and interacting density response functions, respectively, by

$$\begin{aligned} n_{ind}(\vec{r},\omega) &= \int d\vec{r}'\chi^0(\vec{r},\vec{r}';\omega)\phi_{sc}(\vec{r}';\omega) \\ &= \int d\vec{r}'\chi(\vec{r},\vec{r}';\omega)\phi_{ext}(\vec{r}';\omega), \end{aligned} \tag{5-a}$$

where the screened potential is given by

$$\phi_{sc}(\vec{r};\omega) = \phi_{ext}(\vec{r};\omega) + \phi_{ind}(\vec{r};\omega). \tag{5-b}$$

Now, the induced potential $\phi_{ind}(\mathbf{r};t)$ and the induced charge density are related by Coulomb's law[27]

$$\phi_{ind}(\vec{r};t) = \frac{e^2}{(1+\varepsilon)}\int d\vec{r}' \frac{n_{ind}(\vec{r}';t)}{|\vec{r}-\vec{r}'|} \quad (6)$$

We next insert equations(4) and (5) into (6) and make a Fourier transformation, exploiting the translational invariance along the surface; thus we have the Fourier transformed induced potential,

$$\phi_{ind}(q_{\|},\omega;z) = -\frac{32\pi^2 e^3 v_{\perp} e^{q_{\|}z}}{(1+\varepsilon)q_{\|}[q_{\|}^2 v_{\perp}^2 + (\omega - \vec{q}_{\|}\cdot\vec{v}_{\|})^2]}\int_0^{\infty} dz' \int_0^{\infty} dz'' e^{-q_{\|}(z'+z'')}\, \mathrm{Im}\,\chi(q_{\|},\omega;z',z''), \quad (7)$$

where $\chi(q_{\|},\omega;z,z')$ is the reduced density response function, defined as

$$\chi(\vec{r},\vec{r}';\omega) = \int \frac{d\vec{q}_{\|}}{(2\pi)^2} e^{i\vec{q}_{\|}\cdot(\vec{r}_{\|}'-\vec{r}_{\|})}\chi(q_{\|},\omega;z,z') \quad (8)$$

To complete our formal development is now straightforward. The work done on the external electron by the induced charge is evaluated as

$$W = -\int_{-\infty}^{\infty} dt \vec{v}(t)\cdot\nabla\phi_{ind}(\vec{r};t), \quad (9)$$

with $\vec{v}(t) = \vec{v}_{\|} - v_{\perp}|t|\vec{e}_z$.

After some tedious algebra, we find the result

$$W=\int_0^\infty \omega d\omega\{\int \frac{d\vec{q}_{\|}}{(2\pi)^2}\frac{64\pi e^4 v_\perp^2}{(1+\varepsilon)^2[q_{\|}^2 v_{\|}^2+(\omega-\vec{q}_{\|}\cdot\vec{v}_\perp)^2]^2}\int_0^\infty dz\int_0^\infty dz' e^{-q_{\|}(z+z')}\,\mathrm{Im}\chi(q_{\|},\omega;z,z') \tag{10}$$

The work W (total energy loss) on the electron can be reexpressed through the scattering efficiency, ds/dω, as

$$W=\int_0^\infty d\omega\hbar\omega(\frac{ds}{d\omega}) \tag{11}$$

By combining equations(10) and (11) one easily obtains the scattering efficiency for semiinfinite geometry at zero temperature,

$$\frac{ds}{d\omega}=\frac{16e^4 v_\perp^2}{\pi\hbar}\int d^2\vec{q}_{\|}\frac{1}{[q_{\|}^2 v_\perp^2+(\omega-\vec{q}_{\|}\cdot\vec{v}_{\|})^2]^2}\int_0^\infty dz\int_0^\infty dz' e^{-q_{\|}(z+z')}\,\mathrm{Im}\chi(q_{\|},\omega;z,z') \tag{12}$$

Finally, by considering the physical situation of a slab geometry at finite temperature, equation (12) can be generalized as

$$\frac{ds}{d\omega}=\frac{16e^4 v_\perp^2}{\pi\hbar}[1+n(\omega)]\int d^2\vec{q}_{\|}\frac{1}{[q_{\|}^2 v_\perp^2+(\omega-\vec{q}_{\|}\cdot\vec{v}_{\|})^2]^2}\int_0^L dz\int_0^L dz' e^{-q_{\|}(z+z')}\,\mathrm{Im}\chi(q_{\|},\omega;z,z') \tag{13}$$

where $n(\omega)$ is the Bose-Einstein function and L is the thickness of the slab. Comparing equations(13) and (1), we also find the electron energy loss function $P(q_{\|},\omega)$

$$P(q_{\|},\omega)=\frac{8e^2}{(1+\varepsilon)^2}[1+n(\omega)]\int_0^L dz\int_0^L dz' e^{-q_{\|}(z+z')}\,\mathrm{Im}\,\chi(z,z';q_{\|},\omega) \qquad (14)$$

Dynamical Structure Factor

In this section, we shall briefly consider an alternate way of describing the inelastic scattering process in terms of the density response function $\chi(r, r';\omega)$. More generally, in the first Born approximation, the weak interaction between the external electron beam and the medium can be modeled via the differential scattering cross section[20,24,30,31],

$$\frac{d^2\sigma}{d\Omega dE}=\frac{m_p^2|\vec{q}_s|}{(2\pi)^3|\vec{q}_I|}v_{ext}(\vec{q})S(\vec{q},\omega) \qquad (15)$$

where $\mathbf{q}_s$ and $\mathbf{q}_I$ are the scattered and incident momenta while $\mathbf{q}$ and ω are the momentum and energy transfer, respectively. The Fourier transform of the Coulomb interaction is denoted by $v_{ext}(\mathbf{q})$ and m_p is the mass of the external charged particle. All the intrinsic many-body properties are included in the so called dynamical structure factor $S(\mathbf{q},\omega)$. This factor was related to the density response function by Griffin and Harris[32,33]; at finite temperature we have

$$S(\vec{q},\omega) = 2\hbar[1+n(\omega)]\int d\vec{r}\int d\vec{r}' e^{-i\vec{q}\cdot(\vec{r}-\vec{r}')}\,\mathrm{Im}\,\chi(\vec{r},\vec{r}';\omega), \qquad (16)$$

$\chi(r, r';\omega)$ is the density response function as defined in equation(5) and (8). The previous discussion has emphasized that the response function plays a basic role in a variety of physical problems.

Density Response Function

A central quantity in the theory of the homogeneous electron gas is the density-density correlation function[20,34],

$$\chi(\vec{r},\vec{r}';t) = \frac{i\theta(t)}{\hbar} < [\vec{n}(\vec{r},t),\vec{n}(\vec{r}',0)] >_T, \qquad (17)$$

where $n(\mathbf{r},t)$ is the charge density operator, and the angular brackets denote a statistical average of the enclosed operator over a statistical ensemble in equilibrium at temperature T; $\theta(t)$ is a step function with respect to the time t. In the jellium model of a metal or semiconductor surface and quasi-one-dimensional system, the inhomogeneous electron gas can be studied through the same quantity although the problem becomes more complicated due to the lack of translational invariance. For example, the electron-energy-loss function and the inelastic electron scattering cross section which were discussed above, the image potential of a surface[35], and the damping rate of collective excitations[36] can all be related to the density response function $\chi(\mathbf{r},\mathbf{r}';\omega)$, which is the Fourier transform of equation(17) in time. Zangwill and Soven[34] wrote the interacting density response function $\chi(\mathbf{r},\mathbf{r}';\omega)$ explicitly in terms of many-particle quantum states. If $|0\rangle$ and $|f\rangle$ are the exact many-particle ground and final state, respectively, then their result is written as

$$\chi(\vec{r},\vec{r}';\omega)=\sum_{f}\{\frac{<0|\vec{n}(\vec{r})|f><f|\vec{n}(\vec{r}')|0>}{\hbar\omega-(E_f-E_0)+i\delta}-\frac{<0|\vec{n}(\vec{r}')|f><f|\vec{n}(\vec{r})|0>}{\hbar\omega+(E_f-E_0)+i\delta}\}, \quad (18)$$

where the E_f are energy levels and δ a positive infinitesimal. Unfortunately, $\chi(\mathbf{r},\mathbf{r}';\omega)$ cannot be calculated exactly because of the complexity of many-particle states. Yet, we can make one more step without approximation: we can write the density response function of a non-interacting many-particle system $\chi^0(\mathbf{r},\mathbf{r}';\omega)$ exactly since then the non-interacting many-particle states can be built up from single-particle states under the restriction of Fermi-Dirac statistics. So, $\chi^0(\mathbf{r},\mathbf{r}';\omega)$, the same quantity as defined in equation(5), reads[24,34,37-39],

$$\chi^0(\vec{r},\vec{r}';\omega)=\sum_{i,j}(f_i-f_j)\frac{\varphi_i^*(\vec{r})\varphi_j(\vec{r})\varphi_j^*(\vec{r}')\varphi_i(\vec{r}')}{\hbar\omega-(\varepsilon_j-\varepsilon_i)+i\delta}, \quad (19)$$

where f_i and f_j are the Fermi distribution function and the single particle states i and j can be from the selfconsistent Kohn-Sham problem[40,41]of the many-particle ground state within the local-density formalism. $\chi^0(\mathbf{r},\mathbf{r}';\omega)$ will be a very useful function in the approximation procedure used to derive $\chi(\mathbf{r},\mathbf{r}';\omega)$: the random phase approximation or the selfconsistent-field approximation which will be discussed in detail in the next section.

Random-Phase Approximation

Hohenberg, Kohn and Sham[40,41] treated the particle density $n(\mathbf{r})$ as the basic quantity in their theory of the ground-state properties of a many-particle system, the so-

called density-functional formalism. In this formalism, the wavefunctions $\varphi_i(\mathbf{r})$ satisfy the Schrodinger equation,

$$[-\frac{\hbar^2}{2m^*}\nabla^2 + v_{eff}(\vec{r})]\varphi_i(\vec{r}) = \varepsilon_i\varphi_i(\vec{r}) \tag{20}$$

with

$$v_{eff}(\vec{r}) = v(\vec{r}) + e^2\int d\vec{r}'\frac{n(\vec{r})}{|\vec{r}-\vec{r}'|} + v_{xc}(\vec{r}) \tag{21}$$

where $v(\mathbf{r})$ is the electron-nuclear potential, and $v_{xc}(\mathbf{r})$ is the exchange and correlation potential. The particle density $n(\mathbf{r})$ in the above equation is given by,

$$n(\vec{r}) = \sum_i f_i|\varphi_i(\vec{r})|^2 \tag{22}$$

In general, the Kohn-Sham[40] equations defined by equations(20)-(22) must be solved selfconsistently since the unknown wavefunctions $\varphi_i(\mathbf{r})$ are included in the effective potential $v_{eff}(\mathbf{r})$ if one inserts equation(22) into $n(\mathbf{r})$ in equation (21).

Now, when a weak dynamical external potential $\phi_{ext}(\mathbf{r},\omega)$ is applied to a system of charged particles, whose ground state problem is described above, the induced charge density $n_{ind}(\mathbf{r},\omega)$ is given within linear reponse theory by

$$n_{ind}(\vec{r};\omega) = \int d\vec{r}'\chi(\vec{r},\vec{r}';\omega)\phi_{ext}(\vec{r}';\omega) \tag{23}$$

In a selfconsistent theory one also introduces the non-interacting response function $\chi^0(\mathbf{r},\mathbf{r}';\omega)$, defined in equation(19), which satisfies the equation

$$n_{ind}(\vec{r};\omega) = \int d\vec{r}' \chi^0(\vec{r},\vec{r}';\omega)\phi_{sc}(\vec{r}';\omega) \tag{24}$$

Here the screened potential is given by

$$\phi_{sc}(\vec{r};\omega) = \phi_{ext}(\vec{r};\omega) + \phi_{ind}(\vec{r};\omega), \tag{25}$$

and $\phi_{ind}(\mathbf{r};\omega)$ is the induced potential acting on an electron as a consequence of the screening response of the system of charged particles to the external field $\phi_{ext}(\mathbf{r};\omega)$. We can write $\phi_{ind}(\mathbf{r};\omega)$ as a sum of Hartree and exchange-correlation potential:

$$\phi_{ind}(\vec{r};\omega) = \frac{e^2}{\varepsilon}\int d\vec{r}' \frac{n_{ind}(\vec{r}',\omega)}{|\vec{r}-\vec{r}'|} + \frac{dv_{xc}(\vec{r})}{dn(\vec{r})} n_{ind}(\vec{r},\omega) \tag{26}$$

Because equations(23)-(26) have to be solved simultaneously(selfconsistently), we are led to a integral equation for $\chi(\mathbf{r},\mathbf{r}';\omega)$[42-44],

$$\chi(\vec{r},\vec{r}';\omega) = \chi^0(\vec{r},\vec{r}';\omega) + \int d\vec{r}_1 \int d\vec{r}_2 \chi^0(\vec{r},\vec{r}_1;\omega) v(\vec{r}_1,\vec{r}_2)\chi(\vec{r}_2,\vec{r}';\omega), \tag{27}$$

where

$$v(\vec{r}_1,\vec{r}_2) = \frac{1}{\varepsilon}\left[\frac{e^2}{|\vec{r}_1-\vec{r}_2|} + \frac{dv_{xc}(\vec{r})}{dn(\vec{r})}\delta(\vec{r}_1-\vec{r}_2)\right] \tag{28}$$

is the interaction between charged particles. It is important to note that the selfconsistency of the dynamical properties(not the ground state properties) is built into the above integral equation. The induced potential $\phi_{ind}(\mathbf{r};\omega)$is fully specified once a choice has been made for

the exchange-correlation potential in the particle system. In the case that $v_{eff}(\mathbf{r})$(see equation(21)) and (28)) is approximated by averaging electrostatic interaction(the Coulomb interaction) between the electrons, the approximation is called the random-phase approximation(RPA). In the local-density-approximation(LDA), the potential is composed of not only the bare Coulomb but also the exchange-correlation potential as given in equation(28).

Single-Particle and Collective(Spin-Density and Charge Density) Excitations

Single-particle excitations are uncorrelated excitations in which an electron is excited from an initial state below the Fermi level to an empty state above it. The collective excitations involve charge-density and spin-density fluctuations and therefore are dynamically screened by the electron-electron interactions. In linear response theory, the density response function $\chi(\mathbf{r},\mathbf{r}';\omega)$ completely describes the dynamical response of the electron system to an external longitudinal field. The physics of the spin-density excitations (SDE) is best rendered by the response function $\chi^{spin}(\mathbf{r},\mathbf{r}';\omega)$[53] which includes only the spin-dependent exchange-correlation interaction(the direct Coulomb interaction cannot flip the spin), while the single-particle excitations(SPE) and the charge-density excitations(CDE) can be best studied through the noninteraction response function $\chi^{0}(\mathbf{r},\mathbf{r}';\omega)$, and $\chi^{chg}(\mathbf{r},\mathbf{r}';\omega)$, respectively. The latter includes both the direct Coulomb interaction and exchange-correlation.

The integral equation for the charge density response function $\chi^{chg}(\mathbf{r},\mathbf{r}';\omega)$ of the surface problem is given by equation(27). The integral equation for the spin-density response function $\chi^{spin}(\mathbf{r},\mathbf{r}';\omega)$ has the same as equation(27), but the electron-electron

interaction(equation(28)) is replaced by $v(\vec{r}_1,\vec{r}_2)=\frac{1}{\varepsilon}[\delta(\vec{r}_1-\vec{r}_2)dv_{xc}(\vec{r}_1,\vec{r}_2,m)/dm]$ where $m=n_+-n_-$ is the local spin density. We used the Gunnarsson-Lundqvist exchange-correlation energy to evaluate the integral equation.[53]

To summarize our approach, the incorporation of different forms of the electron-electron interaction in the calculation of $\chi(\mathbf{r},\mathbf{r}';\omega)$ leads to three different results:

1) When the energy-loss function $P(q_{||},\omega)$(equation(14)) is evaluated using the noninteraction electron response function $\chi^0(\mathbf{r},\mathbf{r}';\omega)$, the single-particle excitation (SPE) is revealed;

2) The response function $\chi^{spin}(\mathbf{r},\mathbf{r}';\omega)$, which involved only the exchange-correlation potential, predicts the spectrum of spin-density excitations (SDE);

3) The full Coulomb interaction is included in the response function $\chi^{chg}(\mathbf{r},\mathbf{r}';\omega)$. The charge-density excitations (CDE, or plasmons) are found in the calculated spectrum in this case.

The lightscattering method is especially powerful because both spin-density and charge-density excitations can be measured.[45] At small wave vectors the energies of spin-density modes are shifted from single-particle transition energies by exchange-correlation interaction. Charge-density modes have energy shifts due to direct as well as exchange-correlation Coulomb interactions. However, since exchange interactions were expected to be small in GaAs,[45] spin-density excitations were interpreted as single-particle excitation.

Recently, Pinczuk *et al*[45] demonstrated that collective SDE and intersubband SPE as well as CDE of the quasi-two-dimensional electron gas could be measured with inelastic light scattering. The experiments show that exchange-correlation interactions are more important than previously appreciated. We calculated the spectrum of SDE in an accumulation layer of ZnO[53], based on a formalism just described above. The dispersion relation for the SDE lies below the single-particle continuum at small wavevector, while

the CDE appears above the continuum. The dispersion relations of the spin-density and charge-density modes are very similar to those observed in light scattering experiments carried out on GaAs/AlGaAs quantum wells.[45]

CHAPTER 3

ELECTRONIC SUBBAND STRUCTURE AND PLASMON EXCITATIONS OF QUASI-TWO-DIMENSIONAL ELECTRON GAS

Introduction

By quasi-two-dimensional electron gas(Q2DEG) we mean a system in which the electrons are free to move in two spatial dimensions but have their motion constrained in the third dimension. If the range of the confining potential in that dimension is comparable with the de Broglie wavelength we observe new quantum phenomenon: the development of quantum-confined states, with energy levels E_0,E_1,...which are called electronic subbands. The quasi-two-dimensional electron system is reduced to the extreme quantum limit, which is called a two-dimensional electron system[46], when the lowest subband contains all the electrons of the system. The great current interest in Q2DEG is in electron systems of reduced dimensionality, in semiconductors such as GaAs/AlGaAs heterojunctions[47], multiquantum wells[48], inversion layers and accumulation layers[16,17]. Our principal interest here is the systems of electrons in accumulation layers on InAs(110) and ZnO surfaces, and in GaAs/AlGaAs heterostructures.

HREELS and inelastic light scattering have been widely used to characterize the electronic subband properties and the free carrier excitations in semiconductors. Figure 1 shows an example of single-particle transitions in a degenerate quasi-2D electron system. Each confined state of the quantum well is associated with a subband in the two-dimensional wavevector space for electron motion in the plane. Figure 1(a) shows a vertical inter-subband transition between the two lowest subbands($E_{01}=E_1-E_0$). Figure 1(b) represents an intra-subband transition with a wavevector transfer $q_{||}$. Such excitation within one subband is only possible if the wavevector transfer $q_{||}$ is non-zero. Figure 1(c) shows

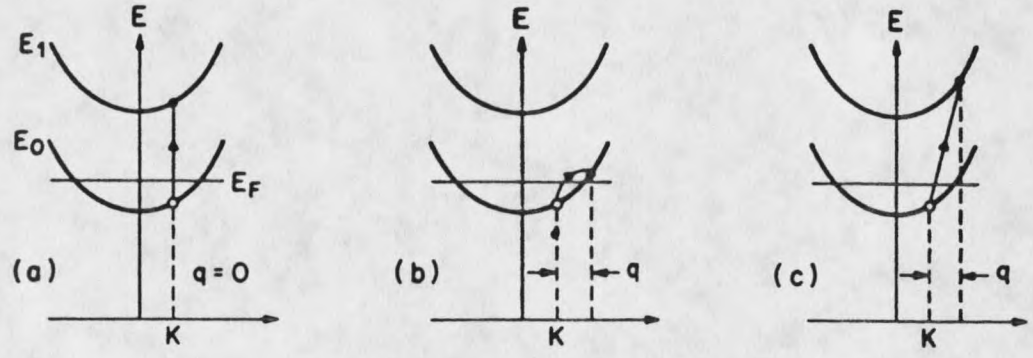

Fig.1 Electronic excitations in quasi-2D systems (a) vertical inter-subband excitation; (b) intrasubband excitation; (c) non-vertical inter-subband excitation.

a non-vertical inter-subband excitation. This excitation has a continum of energies centered at E_{01}. The collective intra-and inter-subband excitations are two-dimensional plasmon oscilations of the electrons parallel and perpendicular to the surface, respectively. Although the collective and single-particle excitations have different energies, we can expect from Figure 1 that the frequencies for collective inter-subband and intra-subband transitions are finite and zero, respectively, when the wavevector transfer $q_{||}$ vanishes. In the next two sections we present detailed calculations of (1)the self-consistent electronic structure of the subbands and (2)the dynamical response of the electron-phonon system, for accumulation layers on InAs[50] and ZnO[51,52]. These systems(especially the latter one) possess a strongly localized electron gas. One would anticipate that such systems exhibit 2D behavior[46,53] because a large majority of the conduction electrons occupy the lowest few subbands, whose spatial extension is much smaller than a typical wavelength involved in HREELS.

Accumulation Layer on InAs (110) Surface

Model and RPA Formalism

A slab of semiconducting material with thickness L large enough to simulate a semiinfinite geometry is considered as our model. In the slab the conduction electrons are treated as a free-electron gas with effective mass m^*, situated in a uniformly charged jellium background with volume charge density n_D due to the donor ions. Auxilliary infinite potential barriers at z=0 and z=L are introduced on both sides of the slab to enforce the boundary condition that the conduction-electron wavefunction vanishes there[10,11]. A positive surface charge density n_S is assumed on both surfaces of the slab. By considering the overall charge neutrality of the slab, if n(z) is the electron density at z and n_{tot} is the integral of n(z) over the slab, we have

$$n_{tot} = n_D L + 2n_s \quad (29)$$

Taking into account the translational invariance in the surface parallel to the slab, the wave function of a conduction electron has the form

$$\varphi_{\vec{k}_\parallel,i}(\vec{x}_\parallel, z) = \frac{1}{A^{1/2}} e^{i\vec{k}_\parallel \cdot \vec{x}_\parallel} \phi_i(z) \quad (30)$$

where $\mathbf{x}_\parallel$ and $\mathbf{k}_\parallel$ are position and wave vector in the surface plane. Inserting equation(30) into the Schrodinger equation appropriate to our model one finds that the electron energy eigenvalues can be written as

$$\varepsilon_i(\vec{k}_\parallel) = \frac{\hbar^2 \vec{k}_\parallel^2}{2m^*} + \varepsilon_i \quad (31)$$

The wavefunctions $\phi_i(z)$ and the energy levels ε_i which correspond to the motion of the electron normal to the surface (z-direction) are related to the electrostatic potential v(z) by the one-dimensional Schrodinger equation

$$\left[\frac{-\hbar^2}{2m^*}\frac{d^2}{dz^2} + v_{eff}(z)\right]\phi_i(z) = \varepsilon_i \phi_i(z) \quad (32)$$

where v(z) is the Hartree potential given by

$$v_{eff}(z) = -\frac{2\pi e^2}{\varepsilon_\infty}\int_0^L [n(z') - n_D]|z - z'|dz' \quad (33)$$

which is the solution of Poisson's equation for charge density -e[n(z)-n_D]. In equation(33) n(z) is the free-carrier density at depth z, given at finite temperature by[10]

$$n(z) = \frac{m^*}{\pi\hbar^2\beta}\sum_i \ln[1+e^{-\beta(\varepsilon_i-\mu)}]|\phi_i(z)|^2 \quad , \tag{34}$$

where $\beta=1/k_BT$ and μ is the chemical potential;the logarithmic factor in equation(34) is essentially the subband occupation number. The chemical potential is determined by the condition of charge neutrality for the slab:

$$n_{tot} = \frac{m^*}{\pi\hbar^2\beta}\sum_i \ln[1+e^{-\beta(\varepsilon_i-\mu)}] \tag{35}$$

Equations(32)-(35) define our self-consistent problem to be solved.

It is convenient to work in Fourier space appropriate to the slab geometry. In order to satisfy the boundary conditions for free wavefunctions, namely $\phi_i(0)=0$ and $\phi_i(L)=0$, we expand the wavefunctions $\phi_i(z)$ in a Fourier sine series:

$$\phi_i(z) = [\frac{2}{L}]^{1/2}\sum_{j=1}^{\infty} b_{ij}\sin(\frac{j\pi z}{L}) \tag{36}$$

The Schrodinger equation can then be transformed into a matrix form[11,36]

$$\sum_{j'=1}^{\infty} M_{jj'}b_{ij'} = \varepsilon_i b_{ij} \qquad i,j = 1,2,3,..., \tag{37}$$

where

$$M_{jj'} = \frac{\hbar^2}{2m^*}[\frac{j\pi}{L}]^2\delta_{jj'} + \frac{2}{L}\int_0^L dz \sin(\frac{j\pi z}{L})\sin(\frac{j'\pi z}{L})v(z) \qquad (38)$$

In our numerical work a basis of 20 to 40 sine waves was found to be adequate to expand the wavefunction. We have performed calculations of the self-consistent potential and charge density for both depletion layers and accumulation layers in GaAs and InAs. The results from our calculations for GaAs are in excellent agreement with those presented previously.[9-13]

The dynamical response of the electron system is described by the RPA formalism developed earlier[10]. The full RPA density response function $\chi(q_{\|},\omega;z,z')$ that describes the nonlocal density response of the slab is obtained by solving the integral equation

$$\chi(q_{\|},\omega;z,z') = \chi^0(q_{\|},\omega;z,z') - \int_0^L dz_1 \int_0^L dz_2 \chi^0(q_{\|},\omega;z,z_1)v_e(q_{\|};z_1,z_2)\chi(q_{\|},\omega;z_2,z') \qquad ,(39)$$

where $v_e(q_{\|};z,z')$ is the two-dimensional Fourier tranform of the electron-electron interaction in the slab, not the Hatree potential of equation(33). We obtained the function $v_e(q_{\|};z,z')$ by solving the Poission equation for an external electron:

$$(\frac{d^2}{dz^2} - q_{\|}^2)v_e(q_{\|};z,z') = -\frac{4\pi e^2}{\varepsilon_\infty}\delta(z-z') \qquad , \qquad (40)$$

together with the usual continuity conditions for $v_e(q_{\|};z,z')$ and $\varepsilon(z)(d/dz)v_e(q_{\|};z,z')$ at z=0,L.

Using standard algebra for obtaining Green's function we have

$$v_e(q_{\|},z,z') = \frac{2\pi e2}{\varepsilon q_{\|}}\{e^{-q_{\|}|z-z'|} + \frac{2}{[(\frac{\varepsilon+1}{\varepsilon-1})e^{2q_{\|}L}-1]}[(\frac{\varepsilon+1}{\varepsilon-1})e^{-q_{\|}L}\cosh(q_{\|}(z+z'-L)) + \cosh(q_{\|}(z-z'))]\} \quad (41)$$

In equation(39) the response function for non-interating electrons is given by

$$\chi^0(q_{\|},\omega;z,z') = \sum_{\alpha,\alpha'} S_{\alpha,\alpha'}(q_{\|},\omega)\phi_{\alpha}(z)\phi_{\alpha}(z')\phi_{\alpha'}(z)\phi_{\alpha'}(z') \quad , \quad (42)$$

where

$$S_{\alpha,\alpha'}(q_{\|},\omega) = 2\int \frac{d^2\vec{k}_{\|}}{(2\pi)^2}\frac{f(E_{\vec{k}_{\|},\alpha}) - f(E_{\vec{k}_{\|}+\vec{q}_{\|},\alpha'})}{E_{\vec{k}_{\|}+\vec{q}_{\|},\alpha'} - E_{\vec{k}_{\|},\alpha} + \omega + i\eta} \quad , \quad (43)$$

and

$$f(E_{\vec{k}_{\|},\alpha}) = \frac{1}{e^{[\beta(\hbar^2\vec{k}_{\|}^2/2m^*+\varepsilon_{\alpha}-\mu)]}+1} \quad (44)$$

is the Fermi-Dirac distribution function. In our numerical work, the parameter η is chosen to be finite but very small and the double summation in equation(42) runs over all the energy levels obtained for the slab.

By using the double-cosine series representation for the response function[36,38],

$$\chi(q_{\|},\omega;z,z') = \sum_{m,n}\chi_{m,n}(q_{\|},\omega)\cos(\frac{m\pi z}{L})\cos(\frac{n\pi z}{L}) \quad , \quad (45)$$

we transform the integral equation(39) for $\chi(q_{\|},\omega;z,z')$ into the matrix equation

$$\chi_{m,n}(q_{\|},\omega)=\chi^{0}_{m,n}(q_{\|},\omega)-\sum_{m',n'}\chi^{0}_{m,m'}(q_{\|},\omega)v_{em'n'}(q_{\|})\chi_{n,n'}(q_{\|},\omega). \tag{46}$$

In the latter equation the coefficients of the double-cosine Fourier transformation of $\chi^{0}(q_{\|},\omega;z,z')$ are given by

$$\chi^{0}_{m,n}(q_{\|},\omega)=\frac{\mu_m\mu_n}{L^2}\sum_{\alpha,\alpha'}S_{\alpha,\alpha'}(q_{\|},\omega)W^{m}_{\alpha,\alpha'}W^{n}_{\alpha,\alpha'}, \tag{47}$$

where the matrix $S_{\alpha,\alpha'}(q_{\|},\omega)$is given by equation(43) and

$$W^{m}_{\alpha,\alpha'}=\frac{1}{2}\sum_{\beta,\beta'}b_{\alpha\beta}b_{\alpha'\beta'}(\delta_{m,\beta-\beta'}+\delta_{m,\beta'-\beta}-\delta_{m,\beta+\beta'}) \tag{48}$$

The matrix element $v_{emn}(q_{\|},\omega)$, in equation(46), is the double-cosine Fourier transform of the electron-electron interaction given in equation(41), or

$$\begin{aligned}v_{emn}(q_{\|},\omega)=\frac{2\pi e^2}{\varepsilon}\frac{1}{q_{\|}^2+(\frac{m\pi}{L})^2}\{&\frac{2L}{(\mu_m\mu_n)^{1/2}}\delta_{mn}-[1+(-1)^{m+n}]\frac{q_{\|}[1-(-1)^m e^{-q_{\|}L}]}{q_{\|}^2+(\frac{n\pi}{L})^2}\\&+(\frac{\varepsilon+1}{\varepsilon-1})e^{q_{\|}L}\frac{q_{\|}}{[(\frac{\varepsilon+1}{\varepsilon-1})^2e^{2q_{\|}L}-1]}\frac{1}{[q_{\|}^2+(\frac{n\pi}{L})^2]}[4\cosh q_{\|}L-2((-1)^m+(-1)^n)]\\&+\frac{q_{\|}}{[(\frac{\varepsilon+1}{\varepsilon-1})^2e^{2q_{\|}L}-1]}\frac{1}{[q_{\|}^2+(\frac{n\pi}{L})^2]}[-4-2((-1)^m+(-1)^n)\cosh q_{\|}L]\}\end{aligned} \tag{49}$$

In our numerical calculations of the electron-energy-loss spectrum, most of the CPU time is required for the calculation of the matrix elements $S_{\alpha,\alpha'}(q_{\|},\omega)$. Without loss of generality, we choose $q_{\|}$ parallel to the y-axis. With this choice $k_{\|x}$ appears only in the

Fermi-Dirac function in $S_{\alpha,\alpha'}(q_{||},\omega)$; the integral with respect to $k_{||x}$ in equation(43) is simply the Fermi-Dirac integral. With reducing the 2-D integral to a 1-D integral, about 45 seconds of CPU time on a VAX 8550 are required to calculate one point on the surface $P(q_{||},\omega)$.

Results and Discussion

It is convenient to adopt thermal units of length and energy[10,11]. In the figures that follow the energy will be scaled in units of k_BT, and the length in units of the thermal de Broglie wavelength $\lambda = (\hbar^2 / 2m^* k_B T)^{1/2}$ or 81.8Å for InAs at room temperature, T=300K. The units of wavevector are λ^{-1}. Thus $\hbar\omega = k_B T$ corresponds to energy 25.9 meV and $q_{||}\lambda=1$ to wavevector 1.22×10^6 cm^{-1}. For InAs, the model parameters we used are $m^*=0.022\ m_0$ when m_0 is the free-electron mass, static dielectric constant $\varepsilon_0=14.9, \varepsilon_\infty=12.3$, and $L=20\ \lambda$. The latter choice corresponds to a slab thickness of 1636 Å, which is large compared with the characteristic width of the accumulation layer, about 100 Å. We emphasize that typical values for $q_{||}\lambda$ in HREELS in the range 0.1 to 0.3. In this range $q_{||}L$ is about 4, so we expect that our slab model is thick enough to simulate a semi-infinite solid; indeed, we find no evidence for a splitting of plasmon modes into even- and odd-parity partners which would signal an interaction between the modes of the opposite sides of the slab.

Figure 2 shows the self-consistent electron density profile computed for a donor density $n_D=1.3 \times 10^{16}$ cm^{-3} and a surface charge density $n_S=1.5 \times 10^{12}$ cm^{-2} on each side of the slab. These parameters were chosen because the free carrier density for the sample studied by HREELS was about 1.3×10^{16} cm^{-3} and because surface charge densities in the range of 10^{11} to 10^{12} cm^{-2} are required to fit the experimental data[15]. We also show the self-consistent potential and the subband energy level diagram at k=0 in Fig.2. We

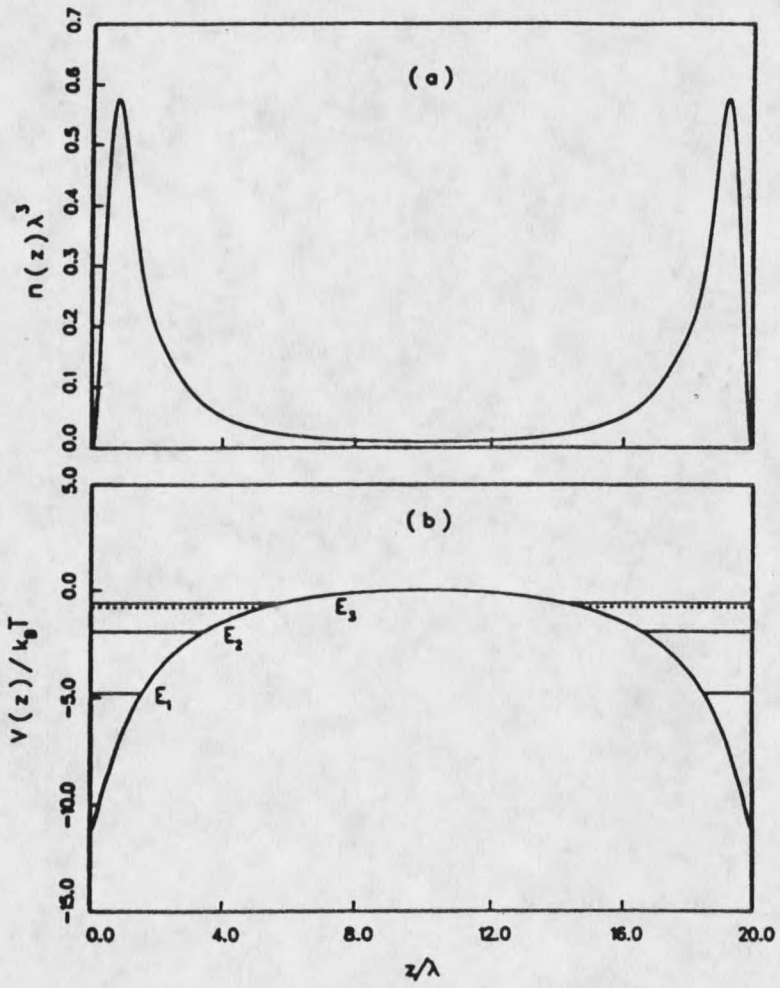

Fig. 2 (a) Self-consistent charge density and (b) potential for InAs accumulation layer; n_D=1.3 x 10^{16} cm^{-3}, n_s=1.5 x 10^{12} cm^{-2}, and L=20 λ. The subband energy levels E_i at k=0 are also shown in (b), as well as the chemical potential μ (dashed line). Dimensionless units are used for the axes.

emphasize that the three lowest subbands are all twofold degenerate;the degeneracy disappears only for bound states very close to the bottom of the bulk conduction band. This behavior indicates that our slab is thick enough to prevent significant overlap between electronic wavefunctions on different sides of the slab. We find that only two subbands are below the Fermi level(E_F=-0.8k_BT), with 70% of the electrons occupying the lowest subband. Also, the maximum value of the electron density for the accumulation layer exceeds that in the bulk by a factor of about 80. Thus we anticipate 2-D character for our computed plasmon modes[53]. The band bending corresponding to the accumulation layer shown in Fig.2(a) is 0.29eV. This agrees reasonably well with the experimental value of 0.22 eV obtained for InAs (110) with a donor concentration of 1.3 x 10^{16} cm^{-3} and a saturation hydrogen exposure[15].

To obtain an explicit expression for the cross-section of inelastic electron scattering we compute the loss function $P(q_{\|},\omega)$ corresponding to energy and wavevector transfers $\hbar\omega$ and $q_{\|}$, respectively. For the slab model the loss function, within the dipole approximation, is given by[10,11]

$$P(q_{\|},\omega)=\frac{8e^2}{|1+\varepsilon|^2}[n(\omega)+1]\int_0^L dz\int_0^L dz' e^{-q_{\|}(z+z')}\,\mathrm{Im}\{\chi(q_{\|},\omega;z,z')\}, \qquad (50)$$

where $n(\omega)$ is the Bose-Einstein distribution function. Figure 3 shows our calculated loss function for different values of the surface wavevector $q_{\|}$ in the range pertinent to HREELS;these results were derived using the charge density shown in Fig.2. At long wavelength, $q_{\|}\lambda \le 0.1$, the loss function contains four narrow peaks, at 0.32, 0.88,1.54 and 3.14 in units of k_BT. The first and second peaks are identified as intrasubband plasmons associated with the second and first subbands, respectively; in particular, the dominant peak in Fig.3 belongs mainly to the lowest subband. The frequency of the latter